11th World Congress on Computational Mechanics (WCCM XI)
5th European Conference on Computational Mechanics (ECCM V)
6th European Conference on Computational Fluid Dynamics (ECFD VI)
E. Oñate, J. Oliver and A. Huerta (Eds)

THE EFFECT OF SEQUENTIAL SOLUTION PROCEDURES IN THE NUMERICAL MODELING OF STIMULATION IN ENGINEERED GEOTHERMAL SYSTEMS

JUSTIN POGACNIK[1], DAVID DEMPSEY[2], SHARAD KELKAR[2], ROB PODGORNEY[3], MIKE O'SULLIVAN[1], AND JOHN O'SULLIVAN[1]

[1]Department of Engineering Science
University of Auckland
Auckland 1010, New Zealand
e-mail: j.pogacnik@auckland.ac.nz

[2]Los Alamos National Laboratory
Los Alamos, New Mexico, USA, 87545
e-mail: d.dempsey@lanl.gov, kelkar@lanl.gov

[3]Idaho National Laboratory
Idaho Falls, ID, USA, 83404
e-mail: robert.podgorney@inl.gov

Key words: Thermo-Hydro-Mechanical Coupled Multiphysics, Permeability Enhancement, Numerical Coupling Procedures, Finite Element Method, Engineered Geothermal Systems

Abstract. In geothermal energy production, reservoir permeability exhibits various degrees of enhancement or degradation with time. These changes are generally attributed to various multiphysics processes such as chemical alteration (dissolution and precipitation), thermal and poroelastic deformation of fractures or the rock matrix, or inelastic failures such as hydrofracking or hydroshearing. If permeability is dependent upon the deformation state of the solid matrix, then a strong feedback is present in the governing differential equations. Few codes are equipped to handle the fully-coupled Thermal-Hydrological-Mechanical (THM) problems in geothermal reservoir simulation. Therefore, separate codes equipped to handle separate differential equations are often loosely coupled to model THM processes.

While previous efforts have investigated numerical coupling procedures in geochemical transport [13], it is not clear what degree of numerical coupling is required to accurately capture the feedback required for permeability enhancement phenomena. In this work, we compare various levels of coupling for modeling Engineered Geothermal System (EGS) well stimulation. Specifically, we address a flow/stress feedback whereby permeability changes as a function of effective stress [8]. The simulations are performed using FEHM

[15], a control-volume finite element THM code that allows for various levels of coupling. Coupled THM modeling is gaining momentum in the geothermal energy sector; a robust analysis of the numerical coupling issues discussed here is imperative in understanding the potential and limitations of this growing field.

1 INTRODUCTION AND BACKGROUND

Numerical modeling has played an important role in understanding the behavior of geothermal systems. In recent years, understanding the phenomenon of permeability enhancement has become important. Permeability can be affected by a number of multiphysics processes such as chemical alteration, thermal and poroelastic deformation of fractures, or inelastic failures (such as hydrofracking or hydroshearing). The mechanically-driven process of permeability alteration can be simulated by coupling the fluid flow and heat energy transport equations to the equations for geomechanics. Very few simulators are equipped to handle the fully-coupled Thermal-Hydrological-Mechanical THM problem. Therefore, separate codes are often coupled to handle different portions of the differential equations.

In computational multiphysics, different differential equations are used to represent different physical processes. The process of solving different portions of coupled differential equations separately is called "operator splitting." Operator splitting has several attractive features for solving coupled differential equations. For example, each stage can be solved using a different numerical technique that is well suited for the specific equation at hand [12]. Also, fully-coupled techniques can require very large linear systems of equations. Only solving for one or two variables at a time can significantly reduce computational costs [13]. In the geothermal sector, often a flow/heat transport solver (such as TOUGH2) is coupled with a solid mechanics code (such as FLAC^{3D} or Abaqus FEA) through the linking and manipulation of input files using scripting [10, 7].

An overview of different operator splitting techniques can be seen in [13]. They explain that there are essentially three different coupling procedures for solving coupled multiphysics systems of equations. The first is termed the "Differential and Algebraic Equation Approach" and is often referred to as the "Globally Implicit Approach" (GIA). The GIA is fully implicit in the sense that all differential equations are simultaneously solved for all unknowns. The second approach is termed "Direct Substitution Approach" or "Sequential Non-Iterative Approach" (SNIA) or sometimes "explicit sequential". This is the most common way of coupling multiple codes/techniques for multiphysics simulations. In this approach one or more variables may be solved for, then those results are passed to another solver to compute another unknown(s). For example, during a simulation, a researcher may use a flow/heat solver to solve two differential equations for fluid pressure and temperatures, then use those results in a solid mechanics solver to determine the stress/displacement field. After all unknowns are computed, the simulation marches forward in time. The third approach is termed the "Sequential Iterative Approach" (SIA) or "implicit sequential" and is the same as the SNIA except that the current time step is repeated either a fixed number of times or until the change in the primary variables is below a certain tolerance.

A number of works have been published that present coupled multiphysics simulations of both hydrofracking and hydroshearing. Some of the hydrofracking studies include models based on damage mechanics [14, 7]. Both of those studies performed numerical simulations using the SIA to couple two different numerical codes. More recent examples of shear stimulation simulations with geothermal application can be found in the literature [5, 11, 2]. The work in [11] did not actually account for time-evolving permeability, but did determine the areas of predicted enhancements. They also performed advanced SIA coupled THM simulations involving two codes. The works of [5] and [2] were performed within a single code, FEHM [15] that performs SNIA coupled THM simulations. The GIA has been used to model coupled THM results for permeability enhancement as a function of effective stress [9]. However none of these works address numerical solution errors that could result in their choice of solution procedure.

While there is a noticeable gap in the geothermal THM literature regarding the change in solution that occurs with different coupling procedures, there has been an extensive amount of work performed in the chemical reaction/transport literature. Efforts have mainly been focused on characterizing different solution techniques and either the associated computational time of each method [13] or theoretical convergence rates [4]. There is also work that seeks to characterize the difference in accuracy between iterative and non-iterative techniques in reactive transport [12]. In THM modeling, there is at least one example where the authors mention their algorithm is capable of both iterative and non-iterative procedures [10]. However, they only provide examples of simulations performed in the non-iterative case.

In this work, we tested two pseudo-1D column problems and a more advanced 3D injection scenario with permeability enhancement to determine the effect that both an iterative and a non-iterative procedure have on the results. We performed these simulations in FEHM which is natively a SNIA code for the isothermal case only. We used FEHM's Python scripting interface PyFEHM, in order to test the SIA coupling. This is the first investigation of different coupling methods in the geothermal energy sector and is imperative due to the increasing popularity in permeability evolution models. We show that iterating in a sequential solve significantly affects the time evolution of the primary variables. This is important because the success of geothermal energy extraction depends on the temperature resource and thermal breakthrough times are of the utmost importance.

2 BALANCE EQUATIONS

2.1 Linear Momentum Balance for the Rock Matrix

In this work, inertial forces in the solid rock matrix are ignored. The linear momentum balance from [1] is written as:

$$\boldsymbol{\nabla} \cdot \boldsymbol{\sigma} + \mathbf{f} = \mathbf{0} \tag{1}$$

where the vector $\boldsymbol{\nabla} \cdot \boldsymbol{\sigma}$ is the spatial divergence of the Cauchy stress tensor (to be formally defined in the next section) and $\mathbf{f}$ a vector of body forces (both external and density related). Note that boldface fonts are used to express matrix and vector quantities. The Cauchy stress can be split into two components to represent the effect of pore fluid pressure on the solid matrix [6, 3]:

$$\boldsymbol{\sigma} = \boldsymbol{\sigma}'' - \alpha p \mathbf{I} \tag{2}$$

where $\boldsymbol{\sigma}''$ is Biots effective stress tensor, α is a constant between 0 and 1, p is the pore fluid pressure, and $\mathbf{I}$ is the identity tensor. The effective stress is defined by

$$\boldsymbol{\sigma}'' = \mathbf{C}^e : (\boldsymbol{\varepsilon} - \boldsymbol{\varepsilon}_T) \tag{3}$$

where $\mathbf{C}^e$ is the fourth order material constitutive tensor, $\boldsymbol{\varepsilon}$ is the strain tensor, ":" represents the double contraction of two tensors, and $\boldsymbol{\varepsilon}_T$ is the thermal strain tensor given by

$$\boldsymbol{\varepsilon}_T = \left(\frac{\beta_s}{3}\right) \Delta T \, \mathbf{I} \tag{4}$$

where β_s is the volumetric coefficient of thermal expansion of the solid and ΔT is the change in temperature from the reference state. In this work, we assume small strain linear elasticity theory applies and thus the fourth order material constitutive tensor is expressed (in indicial notation) as:

$$C^e_{IJKL} = \lambda \delta_{IJ} \delta_{KL} + G \left(\delta_{IK} \delta_{JL} + \delta_{IL} \delta_{JK} \right) \tag{5}$$

where λ and G are the standard lamé parameters.

2.2 Mass Balance

The pore fluid is assumed to be single phase and consist of fully saturated pure water. The mass balance equation can be written (from [3]):

$$\frac{\partial (n \rho_w)}{\partial t} - \boldsymbol{\nabla} \cdot \left[\frac{\boldsymbol{\kappa} \rho_w}{\mu_w} (\boldsymbol{\nabla} p + \rho_w \mathbf{g}) \right] + \dot{m} = 0 \tag{6}$$

where the subscripts w refers to the fluid (water) component, n is the porosity, t is time, $\boldsymbol{\kappa}$ is the permeability tensor, ρ is density, μ is the viscosity, $\mathbf{g}$ is the gravity acceleration vector, and $\dot{m}$ represents mass flow into the system.

2.3 Thermal Energy Balance

To couple thermal effects, we introduce the energy balance equation, also from [3]:

$$\frac{\partial\left[n\rho_w c_w T + (1-n)\rho_s c_s T\right]}{\partial t} - \boldsymbol{\nabla}\cdot\left[\frac{\boldsymbol{\kappa}\rho_w c_w T}{\mu_w}\left(\boldsymbol{\nabla}p + \rho_w\mathbf{g}\right)\right] - \boldsymbol{\nabla}\cdot\{\boldsymbol{\chi}\cdot\boldsymbol{\nabla}T\}] + \dot{h} = 0 \quad (7)$$

where the subscript s refers to the solid (rock) component, c represents the specific heat, T the temperature, $\boldsymbol{\chi}$ is the effective thermal diffusivity of the saturated medium, and $\dot{h}$ is the heat flux into the system.

3 PERMEABILITY ENHANCEMENT

As mentioned earlier, there are a number of permeability enhancement relationships available in the literature. Nathenson [8] provides an overview of a few permeability enhancement relationships (inverse power, cubic power, cubic-log, and exponential) based on effective stress $(\sigma - p)$. In that work, a simple 1D well-to-well analytical flow solution was used to optimize material parameters to match field data taken from the Rosemanowes, U.K. geothermal field. The enhancement relationship favored in Nathenson's analysis (and the one used in this work) was the inverse power relationship given by:

$$\kappa = \frac{\kappa_0}{(1/\sigma_c)(\sigma - p)} \quad (8)$$

where κ is the isotropic scalar permeability, κ_0 is the initial permeability, σ_c is the confining *in situ* stress, and σ is the scalar stress. Nathenson assumed that, at depth, $\sigma = \sigma_c$ for the horizontal component of the principal stress tensor and then equation (8) can be recast as:

$$\kappa = \frac{\kappa_0}{1 - p/\sigma_c}. \quad (9)$$

We implemented this form of the inverse power relationship to test the effect that permeability enhancement had on sequentially coupled solution procedures for a few different boundary value problems. We formulated the permeability tensor as an isotropic tensor such that

$$\boldsymbol{\kappa} = \kappa\mathbf{I}. \quad (10)$$

Notice that the differential equations (6) and (7) both depend on permeability κ. If permeability changes as a result of mechanical deformation in equation (1), then a strong feedback is present and a 'tight' numerical coupling procedure may be necessary to accurately solve the coupled differential equations. The next section will outline our method of implementing the inverse power relationship into sequential solution procedures using the finite element code FEHM.

4 SEQUENTIAL COUPLING PROCEDURE

FEHM is a subsurface multi-phase multi-fluid heat and mass transport code with solid mechanics capabilities. It employs a numerical method called the control volume finite element method to perform a sequential non-iterative solution procedure (SNIA) of first the flow/heat equations using the method of control volumens, then the solid mechanics equations using the finite element method. This work used Python scripting and FEHM's native scripting interface PyFEHM to perform SIA solutions as well. Algorithm 1 gives the pseudocode to perform both SNIA and SIA coupling procedures using FEHM. The important portion for the SIA is to continue to iterate at the current time step if the change in the unknown vector is large. The next section will detail the boundary value problems set up for this study.

Algorithm 1: Pseudocode for sequential coupling procedures

```
· Define geometry and grid
· Define material properties
for t in timesteps do
    · Setup boundary conditions
    · Setup initial conditions
    if SIA then
        while L < 1^-10 do
            · Update permeability (κ) based on effective stress from equation (9)
            · Call FEHM – solve flow/heat followed by displacement with SNIA
            · Compute L2-norm of unknown vector x:
                  L = sqrt((x(t) − x(t − 1))^2)
        end
    else
        · Update permeability (κ) based on effective stress from equation (9)
        · Call FEHM – solve flow/heat followed by displacement with SNIA
    end
end
· Postprocess results
```

5 SIMULATION SETUP

In this work, we tested two pseudo 1D column problems. The first was intended to represent a steady state scenario, while the second was designed to represent a time-dependent pressure drawdown scenario. We also tested a 3D injection scenario to represent fluid injection at depth. This section will detail the material properties chosen for these simulations, then describe the boundary value problems.

5.1 Material Properties

Material parameters were chosen to be representative of reservoir rock in geothermal systems. Table 1 displays the material parameters used in this study.

Table 1: Values of material properties used in this study.

Parameter	Symbol	Value	Units
Rock Density	ρ_s	2500.0	kg/m^3
Young's Modulus	E	72×10^9	Pa
Poisson's Ratio	ν	0.14	-
Rock Coefficient of Thermal Expansion	β_s	5.5×10^{-7}	1/°C
Rock Specific Heat	c_s	1000.0	J/kg °C
Initial Permeability	κ_0	1.0×10^{-14}	m^2
Rock Thermal Conductivity	χ_s	1.5	W/m°C
Biot Coefficient	α	1.0	-

5.2 Steady State 1D Column

The first problem tested was a steady state pseudo 1D column problem. Figure 1 shows the mesh used. The model was three-dimensional with a length of 10 m and width and height equal to 1 m. One element was used in the width and height directions and 40 elements were used in the length direction. Pressure was fixed on the left and right hand sides of the model to 9.99 MPa and 5.0 MPa, respectively. A horizontal traction of 10.0 MPa compression was placed on the left hand side and the bottom, back, and right hand sides were constrained to have zero normal displacement (roller boundary conditions). Temperature was fixed to 15°C in the entire domain.

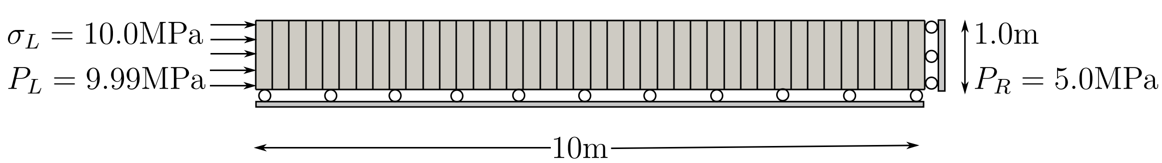

Figure 1: Steady state 1D column geometry.

5.3 Time Dependent 1D Column

The geometry of the time dependent column was similar to Figure 1. The length of the beam was 100 m and the height was 10 m. The left hand traction was set to be 1.0 MPa and the initial pore fluid pressure in the beam was 0.9 MPa. The left hand pressure was then set to be equal to 0.1 MPa to simulate a pressure drawdown scenario. The temperature was again set to 15°C throughout the domain.

5.4 3D Injection Scenario

A 3D injection scenario was set up to simulate water injection into reservoir rock at depth. The domain was a 100 m × 100 m × 100 m cube with 1/8 symmetry and a progressively refined mesh near the injection site near the front bottom corner denoted with p_{inj} in Figure 2. The pressure, p_{top}, and confining stress (acting normal on the top surface), σ_{top}, were set to 8.9 MPa and 23.1 MPa to approximate the conditions at 1000 m depth. A normal traction was placed on the back and right surfaces to be equal to σ_{top}. The bottom, left, and front surfaces were constrained from normal displacement (roller boundary conditions). Gravity was set to act in the vertical direction, resulting in a pore fluid pressure gradient. The injection pressure p_{inj} was set to be 15 MPa over the pressure at the bottom of the domain.

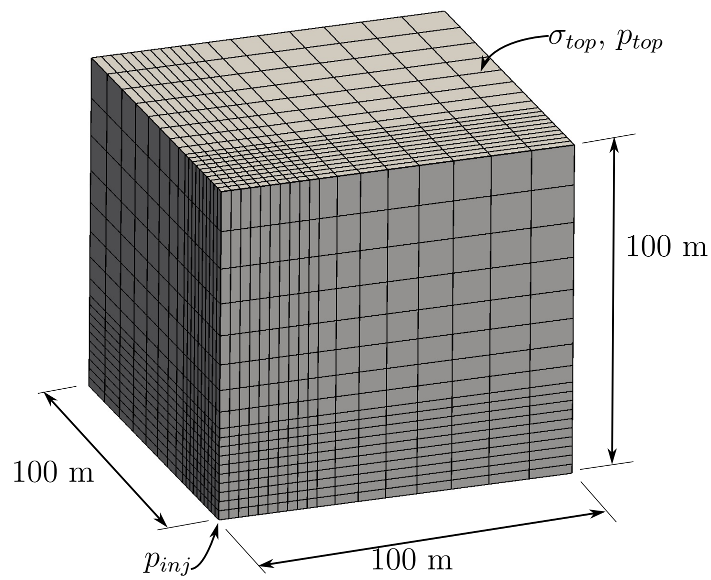

Figure 2: 3D injection scenario column geometry with 1/8 symmetry.

6 NUMERICAL RESULTS AND DISCUSSION

6.1 Steady State 1D Column

In the steady state, both solution procedures converge to the same result. However, the time evolution was different between the methods. Mesh convergence effectively occurred at a refinement level of 40 elements in the horizontal direction. Figures 3 and 4 show the results for pore fluid pressure and log(permeability), respectively, at 100 s, 400 s, and 1000 s of simulation time. The non-iterative approach displays much more change over each time step since permeability is only updated as a result of changes in pressure and stress from the previous time step. After 1000 s, both solution procedures gave the same result.

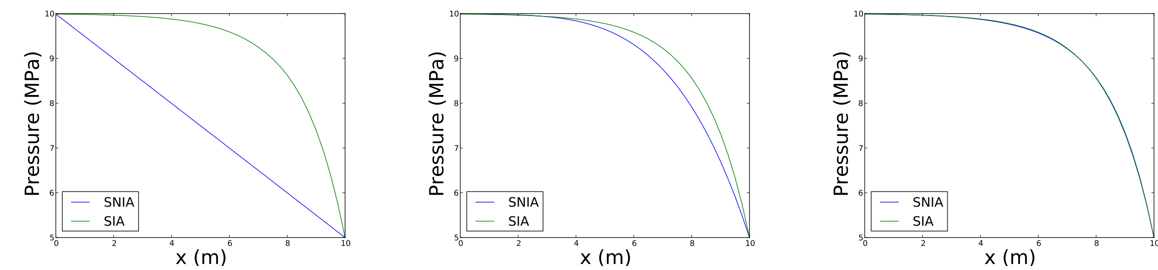

(a) time = 100 s (b) time = 400 s (c) time = 1000 s

Figure 3: The development of the steady steady pressure over time.

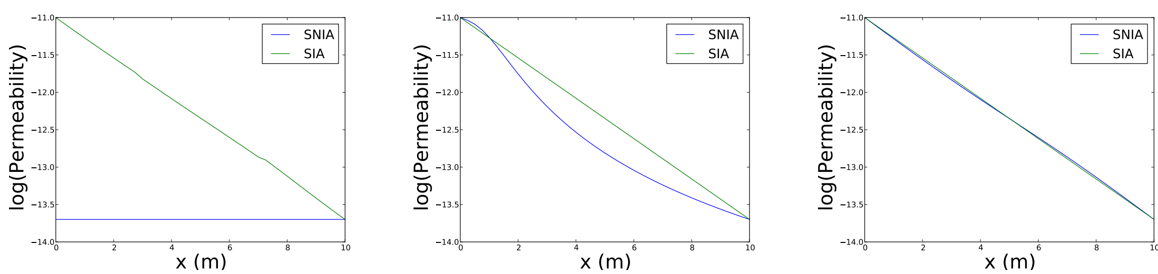

(a) time = 100 s (b) time = 400 s (c) time = 1000 s

Figure 4: The development of log(permeability) for the steady state column over time.

6.2 Time-Dependent 1D Column

The time dependent case was set up to simulate a pressure drawdown scenario. At longer times, pressure should equilibrate to the value at the left hand side of the beam. However, the time evolution of the pressure is important. This requires a numerical procedure that is robust regarding time evolution. Figure 5 displays the pressure evolution for the time dependent problem at 1 s, 2 s, and 3 s of simulation time.

6.3 3D Injection Scenario

Figure 6 displays the result for pressure and the enhanced log(permeability) after 1000 s for the 3D injection scenario. Figure 7 displays the pressure profile results for 10 s, 50

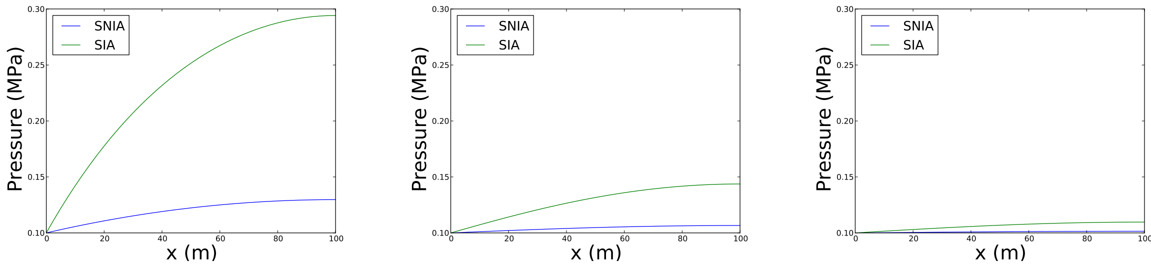

(a) time = 1 s (b) time = 2 s (c) time = 3 s

Figure 5: The development of pressure in the time-dependent column over time.

s, and 100 s along the varying x line where $y = 0$ and $z = 0$ in the domain. The SNIA and SIA are equivalent after 100 s of simulation time for the problem set up used here.

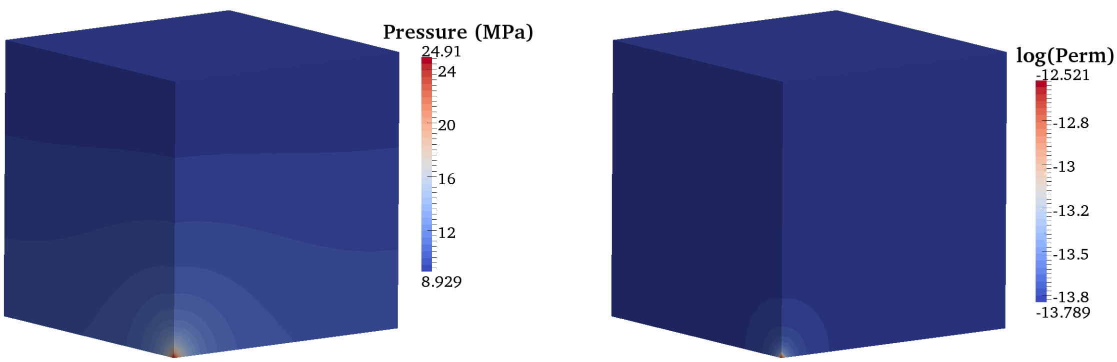

(a) Pressure (b) log(Permeability)

Figure 6: Plot of pressure (a) and log(permeability) (b) after 1000 s of simulation time. Both SNIA and SIA gave the same result at long times. Permeability has increased in the area around the injection site.

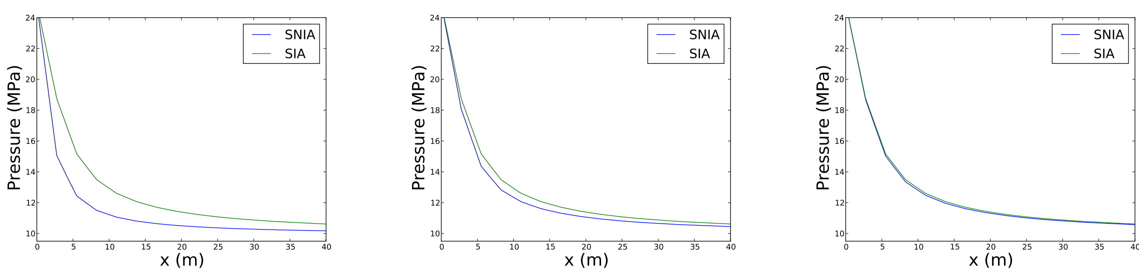

(a) time = 10 s (b) time = 50 s (c) time = 100 s

Figure 7: Plot of 3D injection pore fluid pressure at various times.

7 CONCLUSIONS AND FUTURE WORK

We have set up both sequential non-iterative and iterative solution approaches for a few different problems that undergo permeability enhancement as a result of stress and pore fluid pressure changes in the medium using the code FEHM. This results in a strong feedback from the stress equilibrium equation to the flow and heat transport equations. We have showed that the SNIA and SIA both converge to the same steady state result, but with different time evolutions. This is an important consideration for geothermal applications where pressure drawdown and thermal breakthrough times can impact the economic feasibility of a project. There is an inherit time dependence in all these examples and more work needs to be performed to determine the impact of time step size and time marching procedures.

This work is an initial investigation into coupling procedures and more work needs to be performed. It is essential to use a more appropriate permeability evolution relationship. A number of possibilities exist in the literature and have been mentioned here. All the simulations in this work were isothermal. It is important to include thermal effects in future works to include the significant effect of thermal strain on permeability evolution. Further, it is desirable to compare these sequential solution approaches with a globally implicit approach as well. Since different numerical simulators use different approaches, it would be desirable to perform SNIA, SIA, and GIA all within the same code.

8 ACKNOWLEDGEMENTS

The authors would like to acknowledge GNS of New Zealand for their support of this work.

REFERENCES

[1] Bonet, J. and Wood, R. *Nonlinear Continuum Mechanics for Finite Element Analysis*. Cambridge University Press, Cambridge, U.K. (2008).

[2] Dempsey, D., Kelkar, S., et al. Modeling Shear Stimulation of the Desert Peak EGS Well 27-15 Using a Coupled Thermal-Hydrological-Mechanical Simulator. *47^{th} US Rock Mechanics/Geomechanics Symposium.* (2013) San Francisco, CA. 23-26 June, 2013.

[3] Ingebritsen, S., Sanford, W. and Neuzil, C. *Groundwater in Geologic Processes*. Cambridge University Press, New York. (2006).

[4] Kanney, J., Miller, C. and Kelley, C. Convergence of Iterative Split-Operator Approaches for Approximating Nonlinear Reactive Transport Problems. *Advances in Water Resources* (2003) **26**: 247–261.

[5] Kelkar, S., Lewis, K., Hickman, S., et al. Modeling Coupled Thermal-Hydrological-Mechanical Processes During Shear Stimulation of an EGS Well. *Proceedings, 37th*

Workshop of Geothermal Reservoir Engineering. (2012) Stanford University, Stanford, CA.

[6] Lewis, R. and Schrefler, B. *The Finite Element Method in the Static and Dynamic Deformation and Consolidation of Porous Media.* John Wiley and Sons, (1998),

[7] Lu, Y., Elsworth, D., and Wang, L. Microcrack-based Coupled Damage and Flow Modeling of Fracturing Evolution in Permeable Brittle Rocks. *Computers and Geotechnics.* (2013) **49**: 226–244.

[8] Nathenson, M. The Dependence of Permeability on Effective Stress from Flow Tests at Hot Dry Rock Reservoirs at Rosemanowes (Cornwall) and Fenton Hill (New Mexico). *Geothermics.* (1999) **28**: 315–340.

[9] Pogacnik, J., Leary, P., and Malin, P. Physical/Computational Framework for EGS in situ Fracture Stimulation *Proceedings, New Zealand Geothermal Workshop.* (2012) Auckland, New Zealand.

[10] Rutqvist, J., Wu, Y., Tsang, C., and Bodvarsson, G. A Modeling Approach for Analysis of Coupled Multiphase Fluid Flow, Heat Transfer, and Deformation in Fractured Porous Rock. *International Journal of Rock Mechanics and Mining Sciences.* (2002) **39**: 429–442.

[11] Rutqvist, J., Dobson, P., Garcia, J., et al. Pre-Stimulation Coupled THM Modeling Related to the Northwest Geysers EGS Demonstration Project. *Proceedings, 38th Workshop of Geothermal Reservoir Engineering.* (2013) Stanford University, Stanford, CA.

[12] Valocchi, A. and Malmstead, M. Accuracy of Operator Splitting for Advection-Dispersion-Reaction Problems. *Water Resources Research.* (1992) **28(5)**: 1471–1476.

[13] Yeh, G. and Tripathi, V. A Critical-Evaluation of Recent Developments in Hydrogeochemical Transport Models of Reactive Multichemical Components. *Water Resources Research.* (1989) **25(1)**: 93–108.

[14] Zhou, J., Shao, J., Xu, W. Coupled Modeling of Damage Growth and Permeability Variation in Brittle Rocks. *Mechanics Research Communications* (2006) **33**: 450–459.

[15] Zyvoloski, G. FEHM: A Control Volume Finite Element Code for Simulating Subsurface Multi-Phase Multi-Fluid Heat and Mass Transfer. *Los Alamos National Laboratory Document LAUR-07-3359.* (2007) Los Alamos, NM.